

Can Indigenous Knowledge provide insights into the emerging COVID-19 pandemic:

The role of serpentinization-induced lithospheric long-wavelength magnetic anomalies in mediating the aberrant transformation of biogenic molecules via magnetic catalysis

Author: Moses Turkle Bility¹

Author Affiliation: ¹Department of Infectious Diseases and Microbiology, Graduate School of Public Health, University of Pittsburgh, Pittsburgh, Public Health, 130 DeSoto Street, Pittsburgh, PA 15261.

*Corresponding Author: E-mail: mtbility@pitt.edu, Primary Phone: 412-648-8058, Fax number: 412-383-8926.

Running title: The role of geomagnetic field dynamics in the COVID-19 pandemic.

Grant and funding source: This work is not funded.

Keywords: Geomagnetic field, Lithospheric magnetic field, Coronavirus virus disease, COVID-19, Emerging epidemics and pandemics, Neolithic collapse.

Abstract

In 2019, a severe acute respiratory disease with coupled multiple organ pathologies, namely, Coronavirus Disease 2019 (COVID-19), emerged. The lungs and other organs in this disease exhibit glass-like (hyaline) tissue pathologies with iron oxide deposits, which mimics rock-related mineralization. The impact of significant geological and geophysical perturbations on aberrant mineralization in living organisms has not been explored. Many Indigenous Knowledge systems posit that unseen forces emitted by orogenic structures and modulated by geophysical dynamics play a significant role in health. Here, it is proposed that carbon dioxide-rich water-lithospheric ferromagnesian silicates interactions generate aberrant lithospheric long-wavelength magnetic anomalies (LWMA) via serpentinization, during geologic periods with polar ice melt-induced hydrosphere redistribution, increased atmospheric carbon dioxide, and weakened geomagnetic field intensity. Here, it is also proposed that COVID-19 in humans (and animals) is a pathogenic manifestation of aberrant LWMA-induced magnetic catalysis of silicate/carbonate-like-iron oxides minerals from tissues (carbon-based molecules), gases (dioxygen and carbon dioxide) and metals (iron, magnesium, silicon), and coronavirus from the genome (endogenous viruses), with the virus capable of replication and limited transmission. These COVID-19-LWMAs are generated in tectonic plates with degraded Proterozoic bedrocks and are linked to the refertilization of iron oxides-silicate/carbonate rocks. Thus, severe COVID-19 outbreaks are/will predominately occur on the Eurasian and North American tectonic plates and governed by the diurnal, semiannual (equinoctial maxima, solstitial minima) and quasi-biannual oscillations of the geomagnetic magnetic field intensity (analogous to a vibrating drum head). Furthermore, abnormally high ferromagnetic iron content in humans is the unifying determinant for COVID-19-induced morbidity and mortality.

Introduction

Recent evidence demonstrated that megafauna (including Hominidae) die-offs in the northern hemisphere were associated with geomagnetic field intensity minima [1]. In fact, the Neolithic population collapse, which occurred over a period of approximately 500 years in the mid-Holocene, was temporally coupled to the last geomagnetic field intensity minimum [2-4]. This population collapse disproportionately affected males in the northern hemisphere [5]. M.H. Walczak et al. 2017 demonstrated that this geomagnetic field secular variation in the northern hemisphere in the Holocene epoch is governed by the variable strength of the North American and Eurasian geomagnetic flux lobes at the core-mantle boundary region [6], which in turn are governed by hydromagnetic dynamics [7]. Perturbations in the geodynamo are coupled to mantle perturbations, which modulates changes in lithospheric mantle rock-water interactions and atmospheric carbon dioxide levels [8-10]. The geophysical and geologic conditions of the mid-Holocene are similar to conditions in this era of the Holocene, namely, polar ice melt-induced hydrosphere redistribution [11-13], increased atmospheric carbon dioxide levels [14], and increased weathering (serpentinization) of lithospheric mantle rocks [15, 16] in a severely weakened geomagnetic field [4]. This increased serpentinization of peridotites (ferromagnesium silicates) sequesters excess atmospheric carbon dioxide into lithospheric rock minerals, restoring the carbonate-silicate cycle homeostasis (**Figure 1**) [17, 18]. In late 2019, a severe acute respiratory disease with coupled multiple organ pathologies, termed, Coronavirus disease 2019 (COVID-19) was recorded in humans, resulting in an ongoing pandemic that is disproportionately affecting males in the northern hemisphere [19-21], much like the Neolithic population collapse [5]. The lungs and other organs in COVID-19 exhibit glass-like (hyaline) tissue pathologies with iron oxide deposits [21-26], which mimics

serpentinization-related mineralization; however, the impact of the current severe geological and geophysical perturbations on this pandemic has not been explored. Furthermore, many Indigenous Knowledge systems posit that unseen forces emitted by orogenic structures (and constituent ultramafic rocks) and modulated by geophysical dynamics (Earth-Sun dynamics) play a significant role in health [27-29]. However, a multidisciplinary analysis of this hypothesis, which takes into consideration spin-spin coupling and magnetic catalysis remains to be explored [30-40]. Here, a serpentinization-like aberrant transformation of biogenic molecules (i.e., nucleic acids, carbohydrates, proteins, metals) in the lungs and kidneys of male rats with an emerging severe acute respiratory disease, in the absence of experimental induction, will be examined and compared to COVID-19 pathologies in humans. Additionally, ferromagnetic iron levels in COVID-19 high risk and low risk groups will be compared to determine the role of ferromagnetic iron-associated magnetic catalysis in COVID-19 pathologies. Lastly, the relationship between the spatiotemporal dynamics of severe COVID-19 outbreaks and the lithospheric component of geomagnetic field dynamics will be investigated to establish the role of lithospheric long-wavelength magnetic anomalies in inducing severe COVID-19 outbreaks.

Results

The unrecognized role of serpentinization-induced aberrant lithospheric long-wavelength magnetic anomalies in mediating COVID-19 disease via magnetic catalysis.

It is well-established that geological and geophysical forces maintain the carbonate–silicate geochemical cycle [41-43]. Here, it is proposed that serpentinization of ferromagnesian silicates via interaction with carbon dioxide-enriched water in orogenic belts, results in the generation of aberrant long wave magnetic anomalies during periods of severely weakened

geomagnetic field intensity (**Figure 1**) [44]. Specifically, the generation of iron oxides-silicate/carbonate rock minerals during serpentinization [45] results in the emission of long-wavelength magnetic anomalies. This serpentinization of ferromagnesian silicates (peridotites)

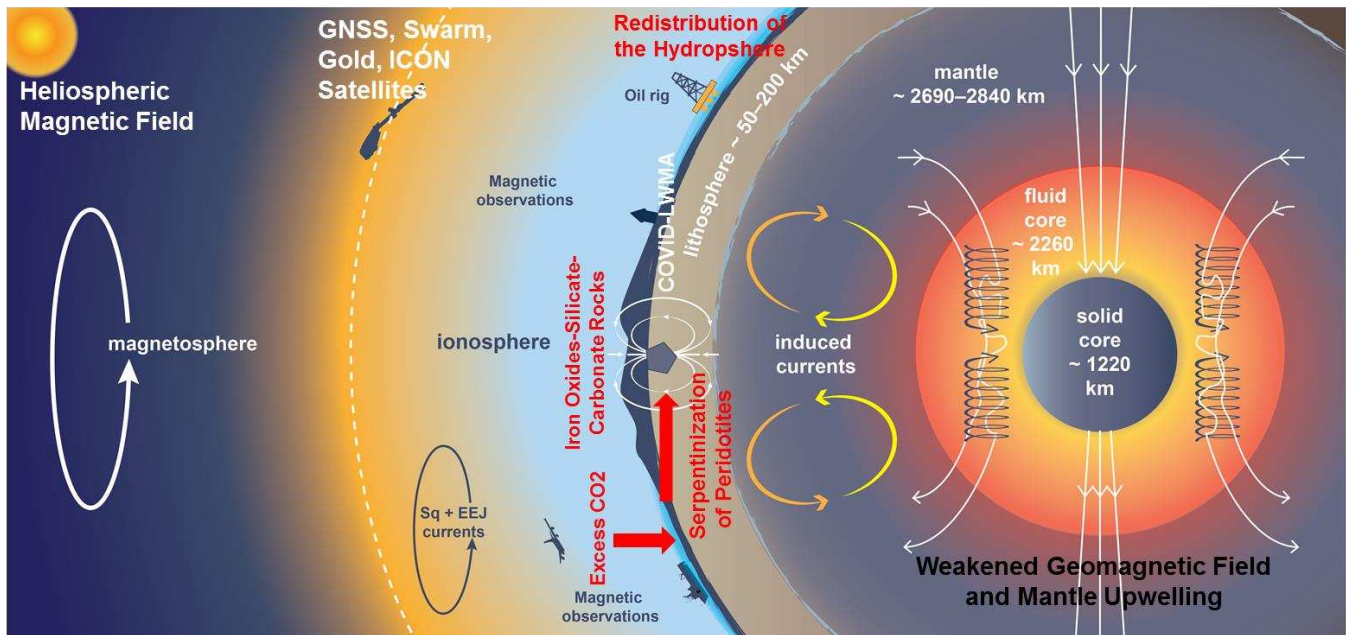


Figure 1: The proposed mechanism of serpentinization-induced lithospheric long-wavelength magnetic anomalies mediated coronavirus disease 2019 (COVID-19) via magnetic catalysis of aberrant biomolecules (viruses) and rock-related mineralization in humans. Excess carbon dioxide (CO₂) in the Earth's atmosphere is modulated via the well-established Carbonate-Silicate geochemical cycle, in which excess atmospheric CO₂ dissolves in water, and this CO₂-rich water reacts with Peridotites to induce serpentinization, especially in the vicinity of orogenic belts on the tectonic plates. The current geologic perturbations involving hydrosphere redistribution (due to polar ice melting), mantle upwelling and excess CO₂ enables increased serpentinization in orogenic belts (i.e. Appalachian and Alpine-Himalayan orogenic belts) and refertilization of the encompassing Precambrian cratons (Proterozoic and Archean cratons). At present, this serpentinization-induced refertilization is associated with the Proterozoic bedrocks in the north hemisphere and the Archean bedrocks in the southern hemisphere, respectively. Here, it is propose that this serpentinization-induced refertilization of the Precambrian bedrocks, generates iron oxides and ferromagnesian-silicate/carbonate rock minerals that emits long-wavelength magnetic anomalies during periods of weakened geomagnetic field intensity, with distinct magnetic anomalies associated with each Precambrian craton. Here, it is hypothesize that COVID-19 outbreaks results from Proterozoic bedrock-LWMAs-induced magnetic catalysis of pathogenic coronavirus and rock-related minerals from biogenic molecules (i.e. endogenous virus, iron, magnesium, silicon, carbohydrates, proteins, lipids) within the human blood and tissues (i.e. lungs and kidneys). We propose that these Proterozoic bedrock-LWMAs (COVID-19-LWMAs) are modulated by the geomagnetic field dynamics (which is coupled to the heliosphere magnetic field dynamics). Therefore, severe COVID-19 outbreaks will predominantly occur in the Eurasia and North American plates, and will oscillate in synchrony with the diurnal, semi-annual (equinoctial maxima, solstitial minima) and quasi-biennial oscillation of the geomagnetic field intensity. Furthermore, magnetometry satellites (Swarm, Gold, ICON) and the global navigational satellite systems (Ionospheric Total Electron Count) in orbit provide a robust means of detecting and tracking (directly or via proxy) the geomagnetic field-spherical harmonics associated with the COVID-19-LWMAs. Airborne and shipborne magnetometry systems also provide means of detecting and tracking those geomagnetic field-spherical harmonics. This figure was modified from an image generated by the National Oceanic and Atmospheric Administration.

during geologic periods with excess atmospheric carbon dioxide levels enables sequestration of the excess atmospheric carbon dioxide in lithospheric rock minerals [41, 43]. Here, it is hypothesized that COVID-19 pathologies in humans and animals result from the aberrant transformation of tissues and metals (iron, magnesium, silicon), and endogenous virus in the human genome via long-wavelength magnetic anomalies-induced magnetic catalysis. Here, it is proposed that the long-wavelength magnetic anomalies (LWMA, waveband >100 kilometers (km) and up to 5000 km) that mediate COVID-19 pathologies are emitted in tectonic plates with Proterozoic bedrocks, during refertilization of the lithospheric rock minerals [44, 46, 47]. Recent evidence in genomics demonstrates the presence of endogenous forms of human viruses, including the so-called emerging viruses, in the genome of humans and many terrestrial animals (including bats) [48-52]. In fact, evidence demonstrates critical roles for endogenous viral genes in normal development and physiology, suggesting that the pathogenic manifestation of viruses could be a result of an aberrant transformation [53]. It is well-established that chemical (including biochemical) reactions are spin restricted [30]. Consequently, altering the spin of reactants in a chemical reaction results in altered rates of reaction and altered products. This spin interaction-mediated catalysis (also called magnetic catalysis) overcomes the mass-isotope restriction of chemical reactions [5, 30, 54]. Here, it is proposed that serpentinization-induced LWMA spin couples with ferrous iron (Fe^{2+}) in hemoglobin in red blood cells, to catalyze ferric iron (Fe^{3+}) formation via interaction with dioxygen (O_2), and subsequently catalyze iron oxides formation via interaction with water molecules (H_2O) in the blood, much like during serpentinization [17, 45, 55]. This magnetic catalysis of iron oxides in red blood cells in COVID-19 results in a rapid depletion of bioavailable dioxygen (anoxic condition), and water molecules (dehydration) [45]. Furthermore,

those iron oxides molecules (i.e., magnetite-black particles) in the red blood cells are ferromagnetic; thus, the ferromagnetic-like red blood cells form a gelatinous-like substance (blood clotting) in the dehydrated blood in vessels, cavities and tissues (lung, skin, heart, kidney, brain, etc.) [56]. Here, it is also proposed that LWMA-ferromagnetic iron spin-spin coupling also mediate the magnetic catalysis ferromagnesian-silicate and -carbonate minerals from biogenic molecules [17, 55, 57, 58]. Over the past six months, an emerging severe acute respiratory disease (~15%, 8 per 55 adult rats; 3 in November 2019, and 5 in late March-early May 2020) was recorded in adult male rats in a humanized rat colony (equal number of male and female immunodeficient rats with or without human hematopoietic-lineage cells and

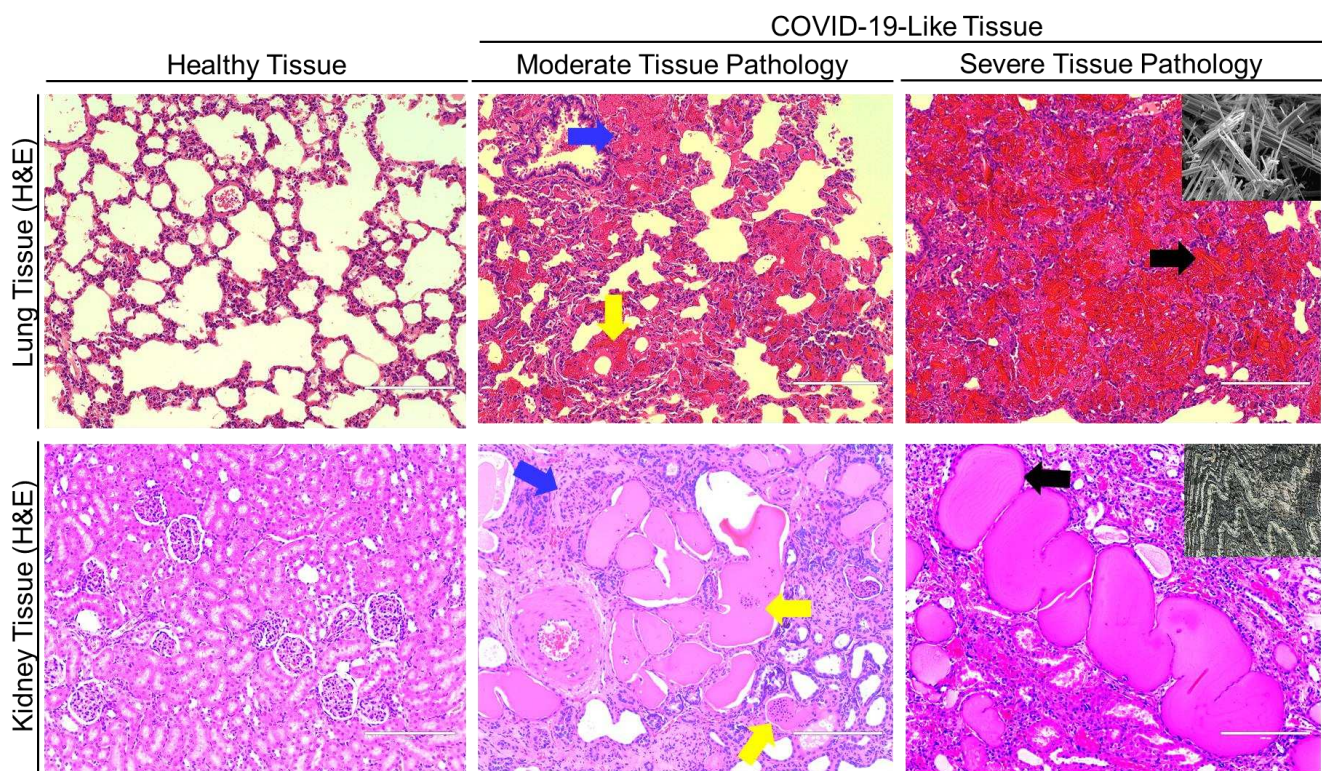


Figure 2: Histopathology analysis of coronavirus disease 2019 (COVID-19)-like disease in a laboratory rat colony in the absence of experimental induction. Histopathological (Hematoxylin and Eosin stain) analysis of lung (top row) and kidney (bottom row) tissues in healthy and COVID-19-like (n=8) rats demonstrates the presence severe lung and kidney pathology, including inflammation and giant cells formation (blue arrow, column 2), and hyaline structures (yellow arrow, column 2), which progresses to significant hemorrhaging and silicate-like minerals (black arrow, column 3). Analysis of silicate rock-minerals (Chrysotile minerals, row 1-column 3; and serpentinite rock, row 2-column 3) demonstrates similar structures in the rat tissues with severe pathology. USGS took the scanning electron micrograph of Chrysotile. Hermann Hammer took the photo of the serpentinite rock, near Geierjoch, Tuxer Alps, Austria (CC0).

lymphoid tissue) in Pittsburgh, Pennsylvania, United States, which temporally overlaps with the emergence of severe acute respiratory diseases in humans (**Supplemental data-videos**).

This disease occurs rapidly, with rats exhibiting excellent health status (normal movement,

breathing, eating, and drinking) in the prior evening, but incapable of breathing by the next morning.

Gross and histological analysis of the major organs in the diseased rats demonstrate significant blood clots and accumulation of black-hemorrhagic patches in the lungs (**not shown**), and glass/quartz-like structures in the lung and kidneys (**Figure 2**). The

glass/quartz-like structures in the kidney mimic the various stages associated with serpentinization-associated rock mineralization

(**Figure 2**) [45]. Tissue iron

analysis in the lung demonstrates the presence of ferric iron (Fe^{3+}) and iron oxides (rust-like) particles coupled with the glass/quartz-like structures and regions with hemorrhagic infiltrates (**Figure 3**). This glass/quartz-like structures and iron oxides deposits in the lung and kidneys in humanized rats is consistent with tissue pathology analysis in COVID-19 deceased individuals

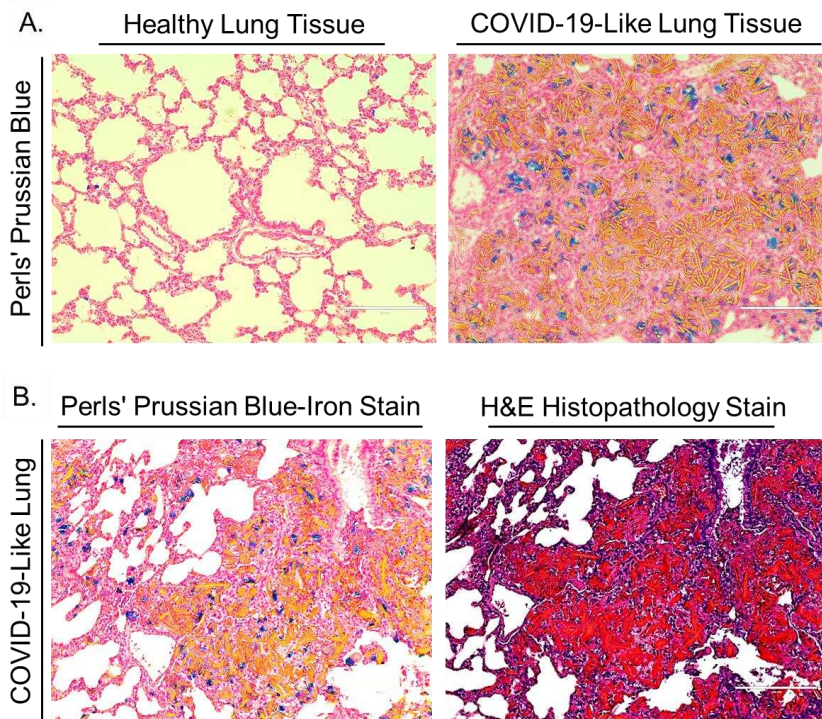


Figure 3: The co-localization of ferromagnetic iron and serpentinization-like mineralization in the lungs of coronavirus disease 2019 (COVID-19)-like disease in a laboratory rat colony in the absence of experimental induction. (A) Perls' Prussian blue-tissue iron analysis in the lungs of laboratory rats with COVID-19-like disease demonstrates the presence of crystal (silicate-like) structures, which co-localized with iron oxides (golden brown-rust; right panel) and ferric iron (Fe^{3+}) (blue stain-right panel); these features were absent in health-control tissue (left panel). (B) These iron oxides-silicate-like structures co-localized with severe hemorrhaging (Bright red color in H&E stain).

[22, 23]. Here, it is also proposed that ferromagnesian-silicate/carbonate minerals serve as a catalytic surface for the magnetic catalysis of pathogenic coronavirus from endogenous viral genes [59-61]. Recent advances in spintronics demonstrate that the application of ferromagnetic material-derived electrons to chiral biomolecules, such as double-stranded deoxyribonucleic acid (dsDNA) results in the efficient generation of spin-polarized currents [62-70]. Additionally, A. L. Buchachenko et al. have demonstrated that magnetic isotope and magnetic field effects modulate DNA synthesis [71]. These developments suggest that interaction of chiral biomolecules (such as dsDNA of endogenous viruses, lipids, carbohydrates, and proteins) on ferromagnesian-silicate/carbonate minerals with a spin coupled-aberrant LWMA could result in magnetic catalysis of aberrant biomolecules, such as pathogenic viruses [72, 73]. Future studies will investigate the presence of SARS-CoV-2 and related coronavirus in the plasma and tissues in our rat colony with COVID-like disease.

Abnormally high ferromagnetic iron content is the unifying determinant of COVID-19 morbidity and mortality.

As stated earlier, ferromagnetic iron is critical for LWMA-mediated magnetic catalysis in COVID-19. Ferromagnetic iron levels (in the blood and tissue stores) are low in children, and increases with age, with the highest levels in the elderly [74-78]. Additionally, males have significantly higher levels of iron compared to females [79]. Furthermore, ferromagnetic iron oxides particulates are ubiquitous in developed countries in the northern hemisphere; thus, another means of increase iron levels in the elderly is environmental-mediated long-term inhalation exposure [80, 81]. Consequently, severe COVID-19 risk is directly proportional to age [82-84], and Male sex is also a major risk factor for severe COVID-19 and death [82].

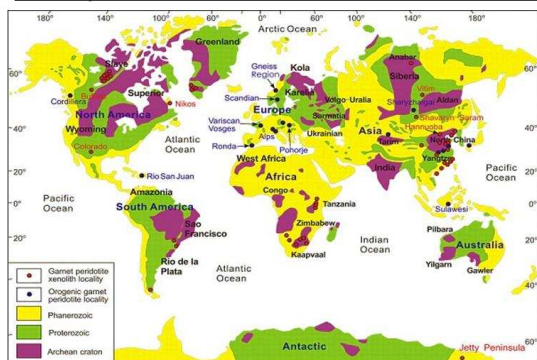
Individuals with metabolic syndrome (i.e., diabetics [85, 86], cardiovascular disease [87, 88], etc.) have a higher risk of COVID-19 due to abnormally high ferromagnetic iron levels in those disease conditions compared to healthy individuals. A retrospective, multicenter cohort study of hospitalized COVID-19 patients, confirmed that abnormally high iron index (serum ferritin levels) is a major determinant of COVID-19 mortality [89].

The nexus between the spatial dynamics of COVID-19 outbreaks and the lithospheric component of the geomagnetic field.

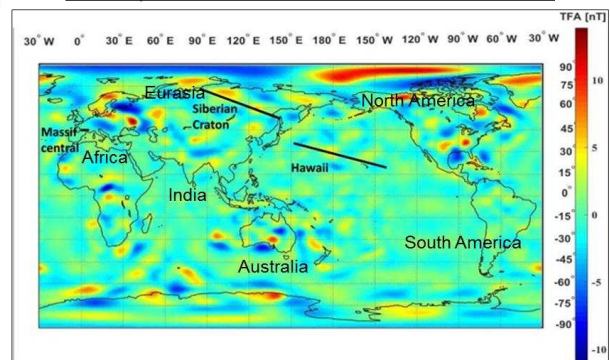
A severe COVID-19 outbreak was first recorded on the Yangtze craton [90] on the eastern portion of the Eurasian plate, and the ensuing severe outbreaks spread westerly on the Eurasian plate, along the Greater Tethyan Eurasian orogenic belt (the Alpine-Himalayan orogenic belt [91-96]). Severe COVID-19 outbreaks predominately co-localize with the troughs of the LWMAAs [44], which are basin regions, with population centers (**Figure 4**). Severe outbreaks spread from the Yangtze River basin (Wuhan, Hubei, China) to basins in Iran in Central Eurasia, the Alpine regions and Spain, and the rest of Western Eurasia, and the Greater Newark basin-Northeastern Appalachian orogenic belt on the northeastern portion of the North American plate [97]. The Greater Tethyan Eurasian orogenic belt has active serpentinization of exhumed peridotites and significant lithospheric long-wavelength magnetic anomalies [44, 91, 95]. The Greater Newark basin-Northeastern Appalachian orogenic belt also has active serpentinization of exhumed peridotites and significant lithospheric long wavelength magnetic anomalies (**Figure 4**) [98-100]. The pandemic also spread easterly, albeit less severe outbreaks in basin regions in South Korea in East Eurasia, the Island of Japan, and the western portion of North America plate (**Figure 4**). Consistent with this bi-

directional (westerly and easterly) travel path of COVID-19 outbreaks from the Yangtze craton [101], the predominant coronavirus strain in the eastern portion of the North American plate is genetically similar to the predominant strain in western Eurasian, while the predominant coronavirus strain on the western seaboard of the North American plate is genetically similar to the predominant strain in eastern Eurasian; despite the fact that travel between Eurasia and North America is a fraction of the travel within North America [102]. Furthermore, the severity of COVID-19 outbreaks on the North American and Eurasian plates is directly proportional to

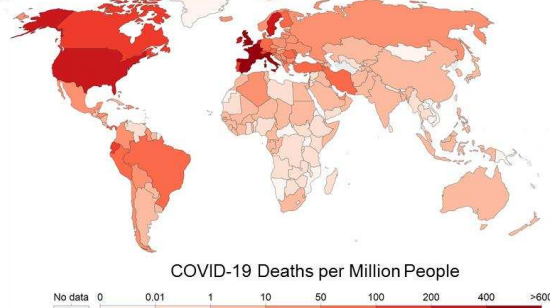
A. Lithospheric Bedrocks of the Tectonic Plates



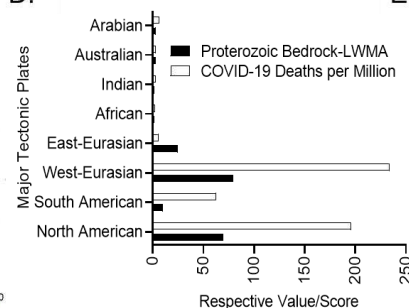
B. Lithospheric-LWMA of the Tectonic Plates



C.



D.



E.

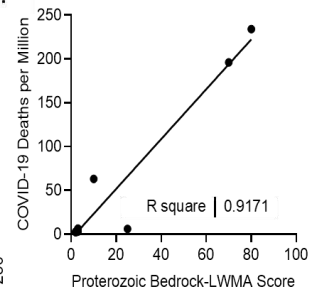


Figure 4: Severe COVID-19 outbreaks is/will be restricted to Proterozoic cratons with long-wavelength magnetic anomalies. Geologic and geophysical analysis by Yan-Jie Tang et al, 2013 and Chijioke M. Idoko et al, 2019 respectively, demonstrate that Proterozoic bedrock (A) in the North American, Eurasian, and South American tectonic plates are associated with long-wavelength magnetic anomalies (B). On the contrary, the long-wavelength magnetic anomalies in the African and Australian plates are associated with Archean bedrocks. Epidemiology analysis of the spatial dynamics of severe COVID-19 outbreaks (deaths per population) by Global Change Data Lab (Our World In Data as of May 21, 2020) demonstrates that countries on the North American (especially eastern United States, not shown), Eurasian (Western Eurasia-Europe), and South American tectonic plates are associated with higher COVID-19 deaths per million people. (D-E) Analysis of the percentage of area covered, and the intensity of Proterozoic bedrock-associated long wavelength magnetic anomalies (Proterozoic Bedrock-LWMA Score), and the severity of COVID-19 outbreaks (Deaths per Million value) on the major tectonic plates (D) demonstrates a direct association (E). Deaths per million values were obtained from John Hopkins University-Coronavirus Resource Center.

the intensity of the Proterozoic bedrock-associated LWMAs (**Figure 4**) [44, 47]. The severity of COVID-19 outbreaks and intensity of the LWMAs are highest in regions in the eastern portion of the North American plate (i.e., Newark basin-Greater New York City area) and the western portion of the Eurasian plate (i.e., Po Valley basin-Lombardy, Italy), and conversely, lowest in regions in the western portion of the North American plate (i.e., Los Angeles basin-Greater Los Angeles area) and the eastern portion of the Eurasian plate (i.e., Mekong River basin) (**Figure 4**) [44, 47]. Regions outside Eurasian and North American plates and lacking Proterozoic bedrock-associated LWMAs (the African, Arabian, Indian, and Australian plates) will not be severe, despite their comparatively weaker public health systems in some of these regions (**Figure 4**) [44, 47]. Furthermore, the governing hydromagnetic perturbations driving the weakening geomagnetic field are predominately restricted to the Eurasian and North American plates [7].

The nexus between the temporal dynamics of COVID-19 outbreaks and the lithospheric component of the geomagnetic field dynamics.

Severe COVID-19 outbreak was first recorded in Eurasia in the early months (January-February) of the vernal solar phase (Eurasian mode), with the temporal severity of the outbreak (growth rate of COVID-19 deaths) in Eurasia peaking in the vernal equinoctial period (late March-late April), and subsequently declining (**Figure 5**). Here, it is proposed that the emergence of COVID-19 outbreaks resulted from the emission of LWMAs that exhibit resonance with ferromagnetic iron in humans, thus enabling spin-spin coupling and magnetic catalysis [73]. The temporal dynamics of the severe COVID-19 outbreaks in Eurasia is synchronous with the temporal dynamics of the ionospheric total electron count (a proxy for the

coupled lithospheric magnetic field dynamics [103, 104]) for the vernal phase in the northern hemisphere, with the peak in the onset of COVID-19 illness associated with the peak daily deaths occurring at the vernal equinox (based on the median time to death of ~3 weeks [89]) (**Figure 5**) [105]. Severe COVID-19 outbreaks in North America also peaked in the vernal equinoctial period (late March-late April) and is currently declining (**Figure 5**) [105]. Here it is proposed that the temporal severity of COVID-19 outbreaks in North American region will be synchronous with the autumnal phase (North America mode) of geomagnetic field dynamics in

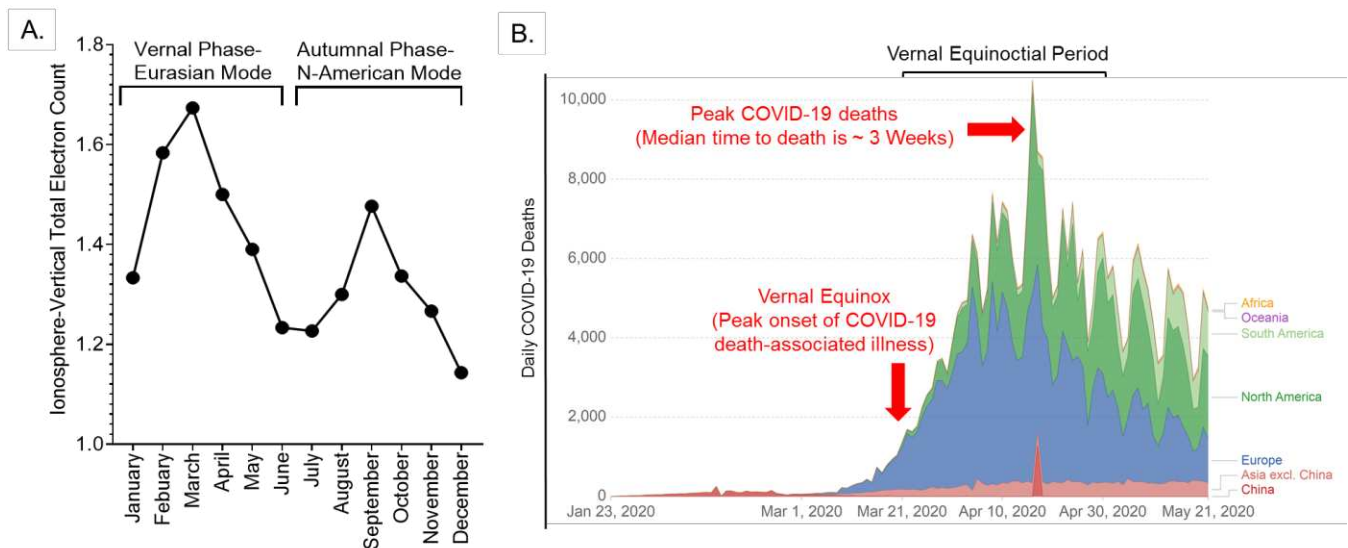


Figure 5: Severe COVID-19 outbreaks is/will be synchronous with the semiannual oscillations of the geomagnetic field intensity. (A) The geomagnetic field is a coupled field, with contributions from the lithosphere and the ionosphere, thus the oscillations of the lithospheric magnetic field and associated long-wavelength magnetic anomalies are synchronous with the ionospheric magnetic field. Analysis of the temporal dynamics of the geomagnetic magnetic field in the northern hemisphere via ionospheric-vertical total electron count measurements from global navigational satellites in 2016 (during a solar minimum) by Parwani, M. et al, 2019, demonstrates the well-established semi-annual oscillation, with two maxima in the equinoctial period (late March-late April, late September-late October) and the two minima in the solstitial period (late June-late July, late December to late January). The vernal phase is designated as the Eurasia mode due to the initiation of the vernal phase-COVID-19 outbreaks in Eurasia, and the autumnal phase is designated the North America mode, due to the projection that severe outbreaks will reemerged first in North America in that period. (B) Epidemiology analysis of the global spatiotemporal dynamics of severe COVID-19 outbreaks (global deaths per region per day) by Global Change Data Lab (Our World In Data as of May 21, 2020) demonstrates a synchronous relationship with geomagnetic field oscillations, with severe COVID-19 outbreaks (global deaths per day) peaking in the equinoctial period of April, and subsequently declining. As of May 21, 2020, the decline in global COVID-19 deaths per day continues. Additionally, the global spatiotemporal dynamics of severe COVID-19 outbreaks mimics a vibrating drumhead, much like the vibrating drumhead dynamics of the geomagnetic field intensity. Note: The median time to death for COVID-19 occurs at ~3 weeks after the onset of illness; thus, there is a ~3 weeks backward shift in the peak (vernal equinox) for the onset of illness associated with the peak daily death.

the northern hemisphere; thus the peak of severe COVID-19 outbreaks in North America is predicted in the autumnal equinoctial period (late September-late October), with the severity of the outbreak subsequently declining (**Figure 5**) [105]. Here it is also proposed that COVID-19 outbreaks in North America in 2019 were misidentified as the vaping-associated severe acute respiratory disease, which affected a relatively small number of people [106-109]. Vaping-associated severe acute respiratory disease exhibited symptomology, lung, and kidney pathologies, with glass-like tissue pathologies and iron oxide-like deposits (black particles), like COVID-19 [106-110]. Furthermore, the temporal dynamics of the vaping-associated severe acute respiratory disease outbreak in North America is comparable to the COVID-19 outbreak, with the epidemic emerging in the vernal equinoctial period (late March-late April), rapidly increasing after the summer solstice, peaking at the autumnal equinox, and subsequently declining thereafter [107, 109]. Therefore, COVID-19 severe outbreaks exhibit a semiannual oscillation, with two maxima in the equinoctial periods (late March-late April; late September-late October), and two minima around the solstices (late June-late July; late December-late January)[105], along with a quasi-biannual oscillation between years, in consistence with the geomagnetic field (and component lithospheric magnetic field) oscillation dynamics (**Figure 5**) [111-113]. In consistence with the hypothesis that severe COVID-19 outbreaks are governed by geomagnetic field dynamics (a vibrating drumhead-like dynamics) [114], the global spatiotemporal dynamics of severe COVID-19 outbreaks mimics a vibrating drumhead-like dynamics, walloping a few countries on the different continents at the same times, despite vast distances between them.

Discussion and Conclusion

The germ theory of viral epidemics/pandemics was first introduced in the early 20th century, displacing the prevailing theory of epidemics/pandemics in most Indigenous knowledge systems across the world [27, 29]. Those indigenous knowledge systems broadly posit that epidemics/pandemics are manifestations of the aberrant transformation of humans via unseen forces emanating from geological structures (i.e., orogenic structures and associated ultramafic rocks) and are governed by geophysical dynamics (i.e., Earth-Sun interactions) [27-29]. Although the germ theory exhibits an explanatory and predictive capacity for many features of the phenomenology of viral epidemics/pandemics, many significant features are unaccounted for in this theory. For example, many respiratory virus-epidemics (i.e., influenza outbreaks) exhibit a spatiotemporal dynamic that is couple to calendar dynamics and associated geographic restriction, despite increased regional/global travel in the 21st century [115-119]. In fact, the current COVID-19 pandemic mimics a vibrating drumhead-like oscillation across the globe, in contrast to the predicted near-simultaneous severe global outbreaks as posited by the germ theory, due to significant increase in global travel over the past century [120, 121]. Furthermore, the phenomenology of the COVID-19 pandemic has contrasted with the germ theory-derived prediction that the severity of the outbreaks (deaths per population) would be relatively higher in regions with relatively weak health systems (i.e., Africa, Southeast Asia), as compared to regions with relatively strong health systems (i.e., North America and Western Eurasian-Europe) [121]. This discordancy cannot be addressed by risk factors (i.e., elderly) associated with mortality and molecular diagnostics capacity. For example, Japan, which lies outside Western Eurasia, has the highest percentage of the elderly population (>65 years old); however, Japan is/did not experience a severe COVID-19 outbreak, despite

receiving a large percentage of travelers from Wuhan and the rest of China [120]. The age distribution within a country is related to the geographic location of the country, with counties in North America and the Western Eurasia-Europe possessing the highest percentage of elders; however, many countries outside those regions, with weak health systems, also have a large population of elders [122]. Although these regions with weak health systems have a relatively lower molecular diagnostic capacity, syndromic surveillance is employed globally [123-127]; thus, deaths due to an emerging severe respiratory disease is captured uniformly across time and different countries, irrespective of national wealth. Another major unanswered question in the germ theory of viral epidemics/pandemics is the origin of the so-called emerging viruses. The current dominant germ theory-derived hypothesis posits that emerging viral outbreaks result from a spill-over of viruses from wildlife into human populations (the zoonosis hypothesis); however, the recent discovery of the genetic fragments of many non-retroviruses, including the so-called emerging viruses, in the genomes of humans and many terrestrial animals raises concerns about the validity of that hypothesis [48, 50, 51]. Calendar-associated dynamics are a manifestation of geophysical dynamics, and those geophysical forces are manifested differently at various geographical locations. Here, we provided evidence supporting the hypothesis, which posts that the COVID-19 pandemic is mediated by serpentinization-induced aberrant LWMA associated with Proterozoic bedrocks. The emergence of these aberrant LWMA is due to severe perturbations in the carbonate-silicate cycle, with the current geologic-geophysical perturbations converting the excess atmospheric CO₂ into ferromagnesian-silicate/carbonate rock minerals [41, 42, 57]. These aberrant LWMA induce magnetic catalysis ferromagnesian-silicate/carbonate-like materials (i.e., hyaline, iron oxides) from biogenic molecules and coronavirus from an endogenous virus in the blood and

tissues via a spin-spin coupling. Furthermore, the resultant coronavirus particles are capable of replication within hosts, and limited transmission across hosts; thus, severe pandemics are predominately mediated by the LWMA. Therefore, the global spatiotemporal dynamics of severe COVID-19 outbreaks will be restricted to regions with Proterozoic bedrocks associated with LWMA and is governed by geomagnetic field dynamics, which mimics a vibrating drumhead-like dynamics [114].

References

1. Channell, J.E.T. and L. Vigliotti, *The Role of Geomagnetic Field Intensity in Late Quaternary Evolution of Humans and Large Mammals*. Reviews of Geophysics, 2019. **57**(3): p. 709-738.
2. Shennan, S., et al., *Regional population collapse followed initial agriculture booms in mid-Holocene Europe*. Nature Communications, 2013. **4**.
3. Batt, C.M., et al., *Advances in archaeomagnetic dating in Britain: New data, new approaches and a new calibration curve*. Journal of Archaeological Science, 2017. **85**: p. 66-82.
4. Nilsson, A., et al., *Reconstructing Holocene geomagnetic field variation: new methods, models and implications*. Geophysical Journal International, 2014. **198**(1): p. 229-248.
5. Karmin, M., et al., *A recent bottleneck of Y chromosome diversity coincides with a global change in culture*. Genome Research, 2015. **25**(4): p. 459-466.
6. Walczak, M.H., et al., *A 17,000 yr paleomagnetic secular variation record from the southeast Alaskan margin: Regional and global correlations*. Earth and Planetary Science Letters, 2017. **473**: p. 177-189.
7. Finlay, C.C., J. Aubert, and N. Gillet, *Gyre-driven decay of the Earth's magnetic dipole*. Nature Communications, 2016. **7**: p. 8.
8. Foley, B.J. and P.E. Driscoll, *Whole planet coupling between climate, mantle, and core: Implications for rocky planet evolution*. Geochemistry Geophysics Geosystems, 2016. **17**(5): p. 1885-1914.
9. Olson, P., *Mantle control of the geodynamo: Consequences of top-down regulation*. Geochemistry Geophysics Geosystems, 2016. **17**(5): p. 1935-1956.
10. Van Der Meer, D.G., et al., *Plate tectonic controls on atmospheric CO₂ levels since the Triassic*. Proc Natl Acad Sci U S A, 2014. **111**(12): p. 4380-5.
11. Marcott, S.A., et al., *A reconstruction of regional and global temperature for the past 11,300 years*. Science, 2013. **339**(6124): p. 1198-201.
12. Park, H.S., et al., *The impact of Arctic sea ice loss on mid-Holocene climate*. Nat Commun, 2018. **9**(1): p. 4571.
13. Golledge, N.R., et al., *Global environmental consequences of twenty-first-century ice-sheet melt*. Nature, 2019. **566**(7742): p. 65-72.

14. Indermuhle, A., et al., *Holocene carbon-cycle dynamics based on CO₂ trapped in ice at Taylor Dome, Antarctica*. Nature, 1999. **398**(6723): p. 121-126.
15. Miriyala, P., et al., *Increased chemical weathering during the deglacial to mid-Holocene summer monsoon intensification*. Sci Rep, 2017. **7**: p. 44310.
16. Gislason, S.R., et al., *Direct evidence of the feedback between climate and weathering*. Earth and Planetary Science Letters, 2009. **277**(1-2): p. 213-222.
17. Lamadrid, H.M., et al., *Effect of water activity on rates of serpentinization of olivine*. Nat Commun, 2017. **8**: p. 16107.
18. Nemani, R., et al., *Recent trends in hydrologic balance have enhanced the terrestrial carbon sink in the United States*. Geophysical Research Letters, 2002. **29**(10): p. 4.
19. Hong, H., et al., *Clinical characteristics of novel coronavirus disease 2019 (COVID-19) in newborns, infants and children*. Pediatr Neonatol, 2020. **61**(2): p. 131-132.
20. Yang, W., et al., *Clinical characteristics and imaging manifestations of the 2019 novel coronavirus disease (COVID-19): A multi-center study in Wenzhou city, Zhejiang, China*. J Infect, 2020.
21. Siordia, J.A., Jr., *Epidemiology and clinical features of COVID-19: A review of current literature*. J Clin Virol, 2020. **127**: p. 104357.
22. Tian, S., et al., *Pulmonary pathology of early phase 2019 novel coronavirus (COVID-19) pneumonia in two patients with lung cancer*. J Thorac Oncol, 2020.
23. Su, H., et al., *Renal histopathological analysis of 26 postmortem findings of patients with COVID-19 in China*. Kidney Int, 2020.
24. Guan, W.J., et al., *Clinical Characteristics of Coronavirus Disease 2019 in China*. N Engl J Med, 2020.
25. Lei, J., et al., *CT Imaging of the 2019 Novel Coronavirus (2019-nCoV) Pneumonia*. Radiology, 2020: p. 200236.
26. Tian, S., et al., *Pathological study of the 2019 novel coronavirus disease (COVID-19) through postmortem core biopsies*. Mod Pathol, 2020.
27. Hewlett, B.S. and R.P. Amola, *Cultural contexts of Ebola in northern Uganda*. Emerg Infect Dis, 2003. **9**(10): p. 1242-8.
28. Darvill, T., *Roads to Stonehenge: A prehistoric healing centre and pilgrimage site in southern Britain*. In A Ranft & Schenkluhn, W (eds), Kulturstraßen als Konzept, 2016. **20 Jahre Straße der Romani**(Regensburg: Schell & Steiner.): p. 155–166.
29. Franks, L.J., *Stone medicine : a Chinese medical guide to healing with gems and minerals*. 2016, Rochester, Vermont: Healing Arts Press. xxiv, 488 pages, 32 unnumbered pages of plates.
30. Buchachenko, A.L. and V.L. Berdinsky, *Spin catalysis as a new type of catalysis in chemistry*. Uspekhi Khimii, 2004. **73**(11): p. 1123-1130.
31. Buchachenko, A.L. and V.L. Berdinsky, *Spin catalysis as a nuclear spin selective process*. Chemical Physics Letters, 1998. **298**(4-6): p. 279-284.
32. Buchachenko, A.L. and V.L. Berdinsky, *Spin catalysis of chemical reactions*. Journal of Physical Chemistry, 1996. **100**(47): p. 18292-18299.
33. Minaev, B.F. and H. Agren, *Spin-Orbit-Coupling Induced Chemical-Reactivity and Spin-Catalysis Phenomena*. Collection of Czechoslovak Chemical Communications, 1995. **60**(3): p. 339-371.
34. Buchachenko, A.L. and V.L. Berdinsky, *Electron spin catalysis*. Chemical Reviews, 2002. **102**(3): p. 603-612.

35. Lassmann, G., et al., *Electron-Spin-Resonance Investigation of Tyrosyl Radicals of Prostaglandin-H Synthase - Relation to Enzyme Catalysis*. Journal of Biological Chemistry, 1991. **266**(30): p. 20045-20055.
36. Khavryuchenko, V.D., O.V. Khavryuchenko, and V.V. Lisnyak, *Effect of spin catalysis in H₂S oxidation: A quantum chemical insight*. Catalysis Communications, 2010. **11**(5): p. 340-345.
37. Buchachenko, A.L., *Mass-independent isotope effects*. J Phys Chem B, 2013. **117**(8): p. 2231-8.
38. Filev, V. and R. Rashkov, *Magnetic Catalysis of Chiral Symmetry Breaking: A Holographic Prospective*. Advances in High Energy Physics, 2010. **2010**: p. 56.
39. Khavryuchenko, O.V., V.D. Khavryuchenko, and D.S. Su, *Spin catalysts: A quantum trigger for chemical reactions*. Chinese Journal of Catalysis, 2015. **36**(10): p. 1656-1661.
40. Gusynin, V.P., V.A. Miransky, and I.A. Shovkovy, *Catalysis of Dynamical Flavor Symmetry Breaking by a Magnetic Field in 2+1 Dimensions*. Phys Rev Lett, 1994. **73**(26): p. 3499-3502.
41. Edson, A.R., et al., *The carbonate-silicate cycle and CO₂/climate feedbacks on tidally locked terrestrial planets*. Astrobiology, 2012. **12**(6): p. 562-71.
42. Caldeira, K., *Continental-pelagic carbonate partitioning and the global carbonate-silicate cycle*. Geology, 1991. **19**: p. 204-6.
43. Brady, P.V., *THE EFFECT OF SILICATE WEATHERING ON GLOBAL TEMPERATURE AND ATMOSPHERIC CO₂*. Journal of Geophysical Research-Solid Earth, 1991. **96**(B11): p. 18101-18106.
44. Idoko, C.M., et al., *The potential contribution to long wavelength magnetic anomalies from the lithospheric mantle*. Physics of the Earth and Planetary Interiors, 2019. **292**: p. 21-28.
45. Huang, R.F., et al., *The production of iron oxide during peridotite serpentinization: Influence of pyroxene*. Geoscience Frontiers, 2017. **8**(6): p. 1311-1321.
46. Mishra, D.C., *Long Wavelength Magnetic-Anomalies from the Lithosphere - Indian Shield and Himalaya*. Tectonophysics, 1984. **105**(1-4): p. 319-330.
47. Tang, Y.J., et al., *Widespread refertilization of cratonic and circum-cratonic lithospheric mantle*. Earth-Science Reviews, 2013. **118**: p. 45-68.
48. Katzourakis, A. and R.J. Gifford, *Endogenous viral elements in animal genomes*. PLoS Genet, 2010. **6**(11): p. e1001191.
49. Horie, M., et al., *Endogenous non-retroviral RNA virus elements in mammalian genomes*. Nature, 2010. **463**(7277): p. 84-7.
50. Feschotte, C. and C. Gilbert, *Endogenous viruses: insights into viral evolution and impact on host biology*. Nat Rev Genet, 2012. **13**(4): p. 283-96.
51. Theze, J., et al., *Remarkable diversity of endogenous viruses in a crustacean genome*. Genome Biol Evol, 2014. **6**(8): p. 2129-40.
52. Russo, A.G., et al., *Novel insights into endogenous RNA viral elements in Ixodes scapularis and other arbovirus vector genomes*. Virus Evolution, 2019. **5**(1).
53. Meyer, T.J., et al., *Endogenous Retroviruses: With Us and against Us*. Frontiers in Chemistry, 2017. **5**.
54. Semenoff, G.W., I.A. Shovkovy, and L.C.R. Wijewardhana, *Universality and the magnetic catalysis of chiral symmetry breaking*. Physical Review D, 1999. **60**(10).

55. Preiner, M., et al., *Serpentinization: Connecting Geochemistry, Ancient Metabolism and Industrial Hydrogenation*. Life (Basel), 2018. **8**(4).
56. Wichmann, D., et al., *Autopsy Findings and Venous Thromboembolism in Patients With COVID-19: A Prospective Cohort Study*. Ann Intern Med, 2020.
57. Rushby, A.J., et al., *Long-Term Planetary Habitability and the Carbonate-Silicate Cycle*. Astrobiology, 2018. **18**(5): p. 469-480.
58. Fredin, O., et al., *The inheritance of a Mesozoic landscape in western Scandinavia*. Nat Commun, 2017. **8**: p. 14879.
59. Holm, N.G., *The significance of Mg in prebiotic geochemistry*. Geobiology, 2012. **10**(4): p. 269-279.
60. Bassez, M.P., *Water near its Supercritical Point and at Alkaline pH for the Production of Ferric Oxides and Silicates in Anoxic Conditions. A New Hypothesis for the Synthesis of Minerals Observed in Banded Iron Formations and for the Related Geobiotropic Chemistry inside Fluid Inclusions*. Origins of Life and Evolution of Biospheres, 2018. **48**(3): p. 289-320.
61. Pedreira-Segade, U., et al., *How do Nucleotides Adsorb Onto Clays?* Life-Basel, 2018. **8**(4): p. 25.
62. Behnia, S., S. Fathizadeh, and A. Akhshani, *DNA Spintronics: Charge and Spin Dynamics in DNA Wires*. Journal of Physical Chemistry C, 2016. **120**(5): p. 2973-2983.
63. Behnia, S. and S. Fathizadeh, *Spintronics in nano scales: An approach from DNA spin polarization*. Scientia Iranica, 2017. **24**(6): p. 3448-3451.
64. Di Ventra, M. and Y.V. Pershin, *SPIN PHYSICS DNA spintronics sees the light*. Nature Nanotechnology, 2011. **6**(4): p. 198-199.
65. Zwolak, M. and M. Di Ventra, *DNA spintronics*. Applied Physics Letters, 2002. **81**(5): p. 925-927.
66. Gohler, B., et al., *Spin Selectivity in Electron Transmission Through Self-Assembled Monolayers of Double-Stranded DNA*. Science, 2011. **331**(6019): p. 894-897.
67. Naaman, R., *Electrons spin and chirality: From molecular spintronics to enantio-recognition*. Abstracts of Papers of the American Chemical Society, 2018. **255**.
68. Naaman, R., *Chirality induced spin selectivity (CISS) effect-chiral molecules for spintronics*. Abstracts of Papers of the American Chemical Society, 2015. **249**.
69. Naaman, R. and D.H. Waldeck, *Spintronics and Chirality: Spin Selectivity in Electron Transport Through Chiral Molecules*. Annual Review of Physical Chemistry, Vol 66, 2015. **66**: p. 263-281.
70. Xie, Z.T., et al., *Spin Specific Electron Conduction through DNA Oligomers (vol 11, pg 4652, 2011)*. Nano Letters, 2012. **12**(1): p. 523-523.
71. Buchachenko, A.L., et al., *Magnetic isotope and magnetic field effects on the DNA synthesis*. Nucleic Acids Res, 2013. **41**(17): p. 8300-7.
72. Liu, M.K., et al., *Spontaneous chiral symmetry breaking in metamaterials*. Nature Communications, 2014. **5**: p. 9.
73. Naaman, R., D.H. Waldeck, and Y. Paltiel, *Chiral molecules-ferromagnetic interfaces, an approach towards spin controlled interactions*. Applied Physics Letters, 2019. **115**(13): p. 4.
74. Xu, J.Z., et al., *Impaired Iron Status in Aging Research*. International Journal of Molecular Sciences, 2012. **13**(2): p. 2368-2386.

75. Picca, A., et al., *Advanced Age Is Associated with Iron Dyshomeostasis and Mitochondrial DNA Damage in Human Skeletal Muscle*. Cells, 2019. **8**(12).
76. Ashraf, A., M. Clark, and P.W. So, *The Aging of Iron Man*. Frontiers in Aging Neuroscience, 2018. **10**.
77. Fleming, D.J., et al., *Dietary factors associated with the risk of high iron stores in the elderly Framingham Heart Study cohort*. American Journal of Clinical Nutrition, 2002. **76**(6): p. 1375-1384.
78. Fleming, D.J., et al., *Iron status of the free-living, elderly Framingham Heart Study cohort: an iron-replete population with a high prevalence of elevated iron stores*. American Journal of Clinical Nutrition, 2001. **73**(3): p. 638-646.
79. Ma, A.G., et al., *Iron Storage in Women is Positively Correlated with Aging and BMI Values*. Faseb Journal, 2016. **30**.
80. Giere, R., *Magnetite in the human body: Biogenic vs. anthropogenic*. Proceedings of the National Academy of Sciences of the United States of America, 2016. **113**(43): p. 11986-11987.
81. Abdul-Razzaq, W. and M. Gautam, *Discovery of magnetite in the exhausted material from a diesel engine*. Applied Physics Letters, 2001. **78**(14): p. 2018-2019.
82. Grasselli, G., et al., *Baseline Characteristics and Outcomes of 1591 Patients Infected With SARS-CoV-2 Admitted to ICUs of the Lombardy Region, Italy*. JAMA, 2020.
83. Team, C.C.-R., *Coronavirus Disease 2019 in Children - United States, February 12-April 2, 2020*. MMWR Morb Mortal Wkly Rep, 2020. **69**(14): p. 422-426.
84. Zheng, F., et al., *Clinical Characteristics of Children with Coronavirus Disease 2019 in Hubei, China*. Curr Med Sci, 2020.
85. Batchuluun, B., et al., *Serum ferritin level is higher in poorly controlled patients with Type2 diabetes and people without diabetes, aged over 55years*. Diabetic Medicine, 2014. **31**(4): p. 419-424.
86. Simcox, J.A. and D.A. McClain, *Iron and Diabetes Risk*. Cell Metabolism, 2013. **17**(3): p. 329-341.
87. Milman, N. and M. Kirchhoff, *Relationship between serum ferritin and risk factors for ischaemic heart disease in 2235 Danes aged 30-60 years*. Journal of Internal Medicine, 1999. **245**(5): p. 423-433.
88. Cheng, W.L., et al., *Determination of serum and erythrocyte iron, serum ferritin, MCH and MCHC related with aged hypertension and coronary heart disease*. Spectroscopy and Spectral Analysis, 1999. **19**(3): p. 383-384.
89. Zhou, F., et al., *Clinical course and risk factors for mortality of adult inpatients with COVID-19 in Wuhan, China: a retrospective cohort study*. Lancet, 2020. **395**(10229): p. 1054-1062.
90. Peng, S.B., et al., *Geology, geochemistry, and geochronology of the Miaowan ophiolite, Yangtze craton: Implications for South China's amalgamation history with the Rodinian supercontinent*. Gondwana Research, 2012. **21**(2-3): p. 577-594.
91. Guillot, S., et al., *Tectonic significance of serpentinites*. Tectonophysics, 2015. **646**: p. 1-19.
92. Giampouras, M., et al., *Geochemistry and mineralogy of serpentinization-driven hyperalkaline springs in the Ronda peridotites*. Lithos, 2019. **350**.
93. Zhao, L., et al., *Evidence for a serpentinized plate interface favouring continental subduction*. Nat Commun, 2020. **11**(1): p. 2171.

94. Hirth, G. and S. Guillot, *Rheology and Tectonic Significance of Serpentinite*. Elements, 2013. **9**(2): p. 107-113.
95. Reynard, B., *Serpentine in active subduction zones*. Lithos, 2013. **178**: p. 171-185.
96. Debret, B., et al., *Three steps of serpentinization in an eclogitized oceanic serpentinization front (Lanzo Massif - Western Alps)*. Journal of Metamorphic Geology, 2013. **31**(2): p. 165-186.
97. Zumla, A. and M.S. Niederman, *Editorial: The explosive epidemic outbreak of novel coronavirus disease 2019 (COVID-19) and the persistent threat of respiratory tract infectious diseases to global health security*. Curr Opin Pulm Med, 2020. **26**(3): p. 193-196.
98. Husch, J.M., *PALISADES SILL - ORIGIN OF THE OLIVINE ZONE BY SEPARATE MAGMATIC INJECTION RATHER THAN GRAVITY SETTLING*. Geology, 1990. **18**(8): p. 699-702.
99. Menke, W., et al., *Crustal Heating and Lithospheric Alteration and Erosion Associated With Asthenospheric Upwelling Beneath Southern New England (USA)*. Journal of Geophysical Research-Solid Earth, 2018. **123**(10): p. 8995-9008.
100. Zakharova, N.V., et al., *New insights into lithology and hydrogeology of the northern Newark Rift Basin*. Geochemistry Geophysics Geosystems, 2016. **17**(6): p. 2070-2094.
101. Stefanelli, P., et al., *Whole genome and phylogenetic analysis of two SARS-CoV-2 strains isolated in Italy in January and February 2020: additional clues on multiple introductions and further circulation in Europe*. Euro Surveill, 2020. **25**(13).
102. Brufsky, A., *Distinct Viral Clades of SARS-CoV-2: Implications for Modeling of Viral Spread*. J Med Virol, 2020.
103. Thebault, E., et al., *The Magnetic Field of the Earth's Lithosphere*. Space Science Reviews, 2010. **155**(1-4): p. 95-127.
104. Prokhorov, B.E., et al., *Simulated vertical electric field data: An estimation from an improved coupling model for the lithosphere-atmosphere-ionosphere system*. Data Brief, 2019. **26**: p. 104513.
105. Parwani, M., et al., *Latitudinal variation of ionospheric TEC at Northern Hemispheric region*. Russian Journal of Earth Sciences, 2019. **19**(1).
106. Butt, Y.M., et al., *Pathology of Vaping-Associated Lung Injury*. N Engl J Med, 2019. **381**(18): p. 1780-1781.
107. Hsuen, Y. and J.S. Brownstein, *Real-Time Digital Surveillance of Vaping-Induced Pulmonary Disease*. N Engl J Med, 2019. **381**(18): p. 1778-1780.
108. Viswam, D., et al., *Respiratory failure caused by lipoid pneumonia from vaping e-cigarettes*. BMJ Case Rep, 2018. **2018**.
109. Hartnett, K.P., et al., *Syndromic Surveillance for E-Cigarette, or Vaping, Product Use-Associated Lung Injury*. N Engl J Med, 2020. **382**(8): p. 766-772.
110. Fels Elliott, D.R., et al., *Giant cell interstitial pneumonia secondary to cobalt exposure from e-cigarette use*. Eur Respir J, 2019. **54**(6).
111. Lyatsky, W. and A.M. Hamza, *Seasonal and diurnal variations of geomagnetic activity and their role in Space Weather forecast*. Canadian Journal of Physics, 2001. **79**(6): p. 907-920.
112. Sebera, J., et al., *On the Observability of the Time-Variable Lithospheric Signal in Satellite Magnetic Data*. Surveys in Geophysics, 2019. **40**(5): p. 1229-1243.

113. Ou, J.M., A.M. Du, and C.C. Finlay, *Quasi-biennial oscillations in the geomagnetic field: Their global characteristics and origin*. Journal of Geophysical Research-Space Physics, 2017. **122**(5): p. 5043-5058.
114. Archer, M.O., et al., *Direct observations of a surface eigenmode of the dayside magnetopause*. Nat Commun, 2019. **10**(1): p. 615.
115. Paul, M., *Seasonality in infectious diseases: does it exist for all pathogens?* Clin Microbiol Infect, 2012. **18**(10): p. 925-6.
116. Fisman, D.N., *Seasonality of infectious diseases*. Annu Rev Public Health, 2007. **28**: p. 127-43.
117. Altizer, S., et al., *Seasonality and the dynamics of infectious diseases*. Ecol Lett, 2006. **9**(4): p. 467-84.
118. Dowell, S.F. and M.S. Ho, *Seasonality of infectious diseases and severe acute respiratory syndrome-what we don't know can hurt us*. Lancet Infect Dis, 2004. **4**(11): p. 704-8.
119. Hirve, S., et al., *Influenza Seasonality in the Tropics and Subtropics - When to Vaccinate?* PLoS One, 2016. **11**(4): p. e0153003.
120. Chinazzi, M., et al., *The effect of travel restrictions on the spread of the 2019 novel coronavirus (COVID-19) outbreak*. Science, 2020. **368**(6489): p. 395-400.
121. Gilbert, M., et al., *Preparedness and vulnerability of African countries against importations of COVID-19: a modelling study*. Lancet, 2020. **395**(10227): p. 871-877.
122. Wang, S., *Spatial patterns and social-economic influential factors of population aging: A global assessment from 1990 to 2010*. Soc Sci Med, 2020. **253**: p. 112963.
123. Daughton, A.R., R. Chunara, and M.J. Paul, *Comparison of Social Media, Syndromic Surveillance, and Microbiologic Acute Respiratory Infection Data: Observational Study*. JMIR Public Health Surveill, 2020. **6**(2): p. e14986.
124. Aghaali, M., et al., *Performance of Bayesian outbreak detection algorithm in the syndromic surveillance of influenza-like illness in small region*. Transbound Emerg Dis, 2020.
125. Salamatbakhsh, M., K. Mobaraki, and J. Ahmadzadeh, *Syndromic Surveillance System for MERS-CoV as New Early Warning and Identification Approach*. Risk Manag Healthc Policy, 2020. **13**: p. 93-95.
126. Smith, S., et al., *Investigating regional variation of respiratory infections in a general practice syndromic surveillance system*. J Public Health (Oxf), 2020.
127. Sokhna, C., et al., *Senegal's Grand Magal of Touba: Syndromic Surveillance during the 2016 Mass Gathering*. Am J Trop Med Hyg, 2020. **102**(2): p. 476-482.